

COMPARATIVE STUDY ON THE PHOTOVOLTAIC PROPERTIES OF DYE-SENSITIZED SOLAR CELLS (DSCs) BASED ON DIFFERENT COUNTER ELECTRODE CONFIGURATIONS

ABSTRACT

In this work we have reported an investigation on *Delonix regia* dye extract as a natural sensitizer for TiO_2 /DSCs assembled with different counter electrodes. Platinum counter electrode was used for one of the DSCs while polyaniline (PANI) was used to replace platinum in the other DSC. The vitriol treated PANI thin film consisted of aniline mixed with potassium dichromate directly reacted on circular graphite foam. The conductivity and Hall coefficient were measured to be $4.894 \times 10^{-1} \Omega^{-1} cm^{-1}$ and $2.061 \times 10^1 cm^3 C^{-1}$ respectively using ECOPIA Hall Effect Measurement System (HMS-3000 Version 3.52). Sequel to this, the DSCs were assembled and characterized using a standard overhead Veeco viewpoint solar simulator equipped with AM 1.5 filter to give a solar radiation of $1000 W/m^2$ and coupled to a Keithley source meter (model 4200SCS) which was connected to the computer via GPIB interface for data acquisition. The overall solar power conversion efficiencies of 0.02% and 0.04% were obtained for TiO_2 -DSC//*Delonix regia* dye//platinum electrode and TiO_2 -DSC//*Delonix regia* dye//PANI electrode respectively. *Delonix regia* dye extract proved to be rather a poor sensitizer as can be seen by the low spectral absorption at lower energies with short circuit current density of $0.10 mA cm^{-2}$ and $0.11 mA cm^{-2}$ respectively. Nevertheless, a 10% decrease in the electron recombination via redox electrolyte and collection at the photoelectrode was observed for TiO_2 -DSC//*Delonix regia* dye//PANI electrode and a 20% increase in the open circuit voltage (V_{oc}) was also observed. Finally, about 37% increase in the fill factor was observed for the TiO_2 -DSC//*Delonix regia* dye//PANI electrode over TiO_2 -DSC//*Delonix regia* dye//platinum electrode. This necessitated approximately 50% increase in the power conversion efficiency for the TiO_2 -DSC//*Delonix regia* dye//PANI electrode over TiO_2 -DSC//*Delonix regia* dye//platinum electrode.

Keywords: *Delonix regia* dye extract, PANI counter electrode, TiO_2 -DSC, short circuit current density, open circuit voltage, fill factor, power conversion efficiency.

1. INTRODUCTION

Dye-sensitized Solar Cells (DSCs) are fast becoming promising alternatives to the conventional silicon based solar cells because of cheap fabrication cost coupled with easy fabrication steps that could lead to a myriad of shapes using flexible substrates to meet the need of various applications [1, 2, 3]. The salient features of a DSC include photoelectrode, photosensitizer, electrolyte (redox couple) and counter electrode [4, 5]. However, the highest efficiency recorded to date is still well below that for the silicon based solar cells [6, 7, 8]. The major factor

responsible for low energy conversion efficiency is the competition between generation and recombination of photo-excited carriers in DSCs [1]. As such, most of the efforts made so far are targeted toward the synthesis of new nanostructured working and counter electrodes to ameliorate this setback [9, 10, 11, 12, 13]. Sequel to this, surface modification of TiO_2 was studied by depositing SrTiO_3 on its surface to form a core-shell structure in order to shift its conduction band upward closer to the excited state of the coated dye causing enhancement in the open-circuit voltage [11]. As for the counter electrode, the research on the 3-dimensional nanostructure is currently ongoing but the increased surface area offers more locations for I^{3-} reduction and also shortens the redox couple diffusion length. As a follow-up to this, a vertically aligned carbon nanotube counter electrode was fabricated for use in DSC and this led to an increased short-circuit current compared to that obtained using the conventional platinum counter electrode [12]. Even though, it is well-known that redox couple reduction at the counter electrode is not the rate-determining step in the operation of a DSC, efforts are still ongoing to improve the performance of the counter electrodes, dyes and electrolytes [7, 8, 14, 15]. Herein we report a carefully structured polyaniline (PANI) thin film as counter electrode for use in DSC so as to improve its energy conversion efficiency. The film consisted of aniline mixed with potassium dichromate and reacted on circular graphite foam directly to preserve the stoichiometry and prevent over oxidation of the aniline which would have reduced the conductivity. The vitriol treated PANI is a p-type semiconducting polymer with low mobility and conductivity values. The sign and value of the Hall coefficient also validated the nature of the carriers with $3.029 \times 10^{17} \text{ cm}^{-3}$ as the measured bulk concentration and thus can function as efficient counter electrode. In our previous study, we developed and characterized a DSC based on TiO_2 nanoparticles coated with delonix regia and the overall solar power conversion efficiency of 0.02% and a maximum current density of 0.10 mA cm^{-2} were obtained. Typically, low peak absorption coefficient, small spectra width and very low power conversion efficiency of this DSC boosted additional studies oriented; on one hand, to the use of modified photoelectrode and on the other hand, we hope to improve the power conversion efficiency with use of a semiconducting polymeric counter electrode. Sequel to this, two (2) DSCs; one with platinum counter electrode and the other with PANI counter electrode, were assembled and characterized using a standard overhead Veeco viewpoint solar simulator equipped with AM 1.5

filter to give a solar radiation of 1000 W/m^2 and coupled to a Keithley source meter (model 4200SCS) which was connected to the computer via GPIB interface for data acquisition.

2. MATERIALS AND METHODS

Titanium isopropoxide, Titanium nanoxide, acetylacetonate, ethanol, isopropanol, fluorine doped tin-oxide (FTO) conducting glass [11.40 ohm/m^2 , $(1.00 \times 1.00) \text{ cm}^2$], electrolyte (iodolyte-AN-50), sealing gasket (surlyn-SX1170-25PF), and screen-printable platinum catalyst, (Pt-catalyst T/SP) all were obtained from SOLARONIX. Dye extract was obtained from the natural product (*Delonix regia*). A mixture of 0.3M of titanium isopropoxide, 1.2M acetylacetonate and isopropanol was spin coated three (3) times with different concentrations sequentially as blocking layer on the pre-cleaned fluorine doped tin-oxide (FTO) conducting glasses and sintered at 150°C for four minutes each time the deposition was made. Subsequently, a paste of titanium nanoxide in propanol in the ratio 1:3 was screen printed on the three (3) fluorine doped tin-oxide (FTO) conducting glasses and allowed to dry at 125°C in open air for 6 minutes. The FTO/TiO₂ glass electrodes were sintered in a furnace at 450°C for 40 minutes and allowed to cool to room temperature to melt together the TiO₂ nanoparticles and to ensure good mechanical cohesion on the glass surface. Fresh leaves of *Delonix regia* were crushed into tiny bits and boiled in 75ml of deionized water for 15 minutes. The residue was removed by filtration and the resulting extract was centrifuged to further remove any solid residue. The dye extract was used directly as prepared for the construction of the DSCs at room temperature. A scattering layer of TiO₂ was also deposited on the TiO₂ electrodes before the electrodes were immersed (face-up) in the natural dye extract for 18h at room temperature for complete sensitizer uptake. This turned the TiO₂ film from pale white to sensitizer colour. The excess dye was washed away with anhydrous ethanol and dried in moisture free air. The thickness of TiO₂ electrodes and the deposited scattering layers was determined using Dekker Profilometer. Surface morphology of the screen-printed TiO₂ nanoparticles was observed using EVOI MA10 (ZEISS) multipurpose scanning electron microscope operating at 20 kV employing secondary electron signals while the corresponding Energy Dispersive Spectra (EDS) were obtained using characteristic x-rays emitted by TiO₂ nanoparticles. The X-ray diffraction (XRD) pattern of the screen-printed TiO₂ nanoparticles at room temperature was recorded using X-ray Diffractometer; Panalytical Xpert-

Pro, PW3050/60, operating at 30mA and 40kV, with monochromatic Cu-K α radiation, of wavelength $\lambda = 1.54060\text{\AA}$. A scanned range $3-80.00553^\circ 2\theta$, with a step width of 0.001° was used. The pattern was analyzed and the peaks were identified using ICDD data file (01-075-8897). The UV-Visible (UV-Vis) absorption measurements of the dye extract and the dye extract on the screen printed TiO₂ electrodes were carried out with Avante UV-VIS spectrophotometer (model-LD80K). From these measurements, plots for the absorbance, Light Harvesting Efficiency (LHE) and molar extinction coefficient versus the wavelengths of interest were obtained using the relevant expressions from [16]. Few drops each of aniline and K₂Cr₂O₇ were coated on graphite foam by gently turning the graphite foam by hand to fabricate alternative counter electrode. The mixture was grown directly on graphite foam to preserve the stoichiometry. After the process, a greenish thin film of polyaniline (PANI) was formed atop the graphite foam signifying that there was no over oxidation of the aniline which would have reduced the conductivity. After drying, the surface of the counter electrode was thereafter rinsed using vitriol (H₂SO₄). Subsequently, the electrical characteristics of the semiconducting PANI deposited on soda lime glass following the above process were determined using ECOPIA HALL EFFECT MEASUREMENT SYSTEM (HMS-3000 VERSION 3.52). A DSC of 0.52cm^2 active area was assembled by sandwiching a surlyn polymer foil of $25\mu\text{m}$ thickness as spacer between the photoelectrode and the platinum counter electrode and then hot-pressed at 80°C for 15s. A few drops of electrolyte were introduced into the cell assembly via a pre-drilled hole on the counter-electrode and sealed using amosil sealant. In order to have good electrical contacts, a strip of wire was attached to both sides of the FTO electrodes. Similarly, in assembling the modified DSC, the same process as above was adopted but instead of platinum counter electrode PANI coated on circular graphite foam was clamped onto the photoelectrode to form a monolithic cell of 0.78cm^2 active area. Finally, the DSCs were subjected to current-voltage characterization using a standard overhead Veeco viewpoint solar simulator equipped with Air Mass 1.5 (AM 1.5) filter to give a solar radiation of 1000 W/m^2 and coupled to Keithley source meter (model 4200SCS) which was connected to the computer via GPIB interface for data acquisition. Subsequently, the working electrode and counter electrode of the DSC were connected in turn to the positive and negative terminals of the digital Keithley source meter respectively. The bias was from short circuit to open circuit and was obtained automatically using LabVIEW software from National Instruments Inc, USA. From the data, $I-V$ curves were

plotted in real time for the DSCs under illuminated condition. Following this, the photovoltaic parameters viz; the open circuit voltage (V_{oc}) and short circuit current (I_{sc}) were obtained from the I - V curves for the cells. The fill factor (FF) and the power conversion efficiency for the cells were obtained using the following relations:

$$FF = \frac{P_m}{V_{oc} \cdot I_{sc}} \text{ and } \eta = \frac{FF \cdot V_{oc} \cdot J_{sc}}{I_{in}} \quad (1)$$

3. RESULTS AND DISCUSSION

The image presented in Figure 1 obtained using characteristic x-rays emitted by TiO_2 nanoparticles was observed at a magnification of 83.04kX. The uniform contrast in the image revealed TiO_2 to be practically isomorphic with titanium and oxygen being the dominant elements with concentration of about 99.9% as depicted in the EDS spectra (Figure 1b). The morphology of TiO_2 nanoparticles is such that the particles are closely packed and spherical in shape. The average diameter of the particles is in the range of 25-40nm reflecting that TiO_2 nanoparticles are transparent and suitable for DSC application. The thickness of TiO_2 on the FTO conducting glass determined using Dekker Profilometer was found to be 5.2 μm for each photoelectrode and that of the deposited scattering layers was found to be 1 μm . The XRD pattern revealed the compound name for the TiO_2 electrode to be anatase syn., and the structure type is tetragonal with 3.53217 \AA as the d -spacing for the most prominent peak, $2\theta=25.2139^\circ$ (ICDD data file: 01-075-8897). Other prominent peaks occur at $2\theta= 37.7883^\circ, 48.0463^\circ, 53.9110^\circ, 55.0481^\circ, 62.7104^\circ$ and 75.1376° with d -spacing $d= 2.38075 \text{ \AA}, 1.89370 \text{ \AA}, 1.70073 \text{ \AA}, 1.66826 \text{ \AA}, 1.48160 \text{ \AA}$ and 1.26338 \AA .

In figure 2, the dye extract exhibits absorption maxima slightly above 400nm and the most prominent shoulder occur slightly above 500nm. But upon sensitization on TiO_2 , there was a decrease in the absorption maxima and shoulder with a cut off slightly above 600nm.

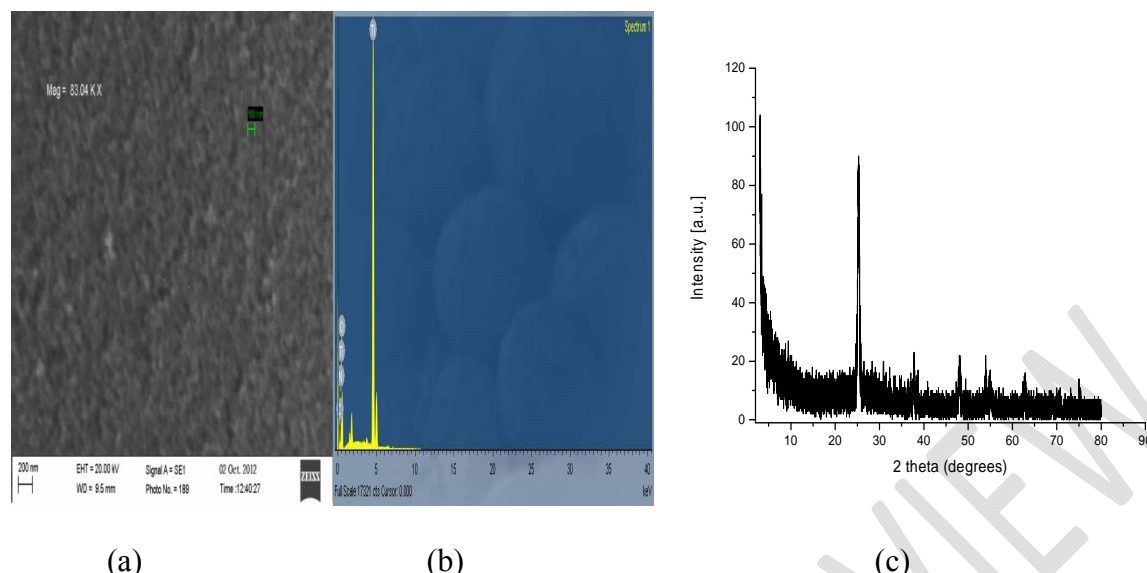


Figure 1: TiO_2 structural characteristics: (a) Surface morphology, (b) EDS spectra and (c) XRD pattern for the screen printed TiO_2 .

It was reported that chemisorption of anthocyanins on TiO_2 was due to alcoholic bound protons which condense with the hydroxyl groups present at the surface of nanostructured TiO_2 [15]. Such attachment to the TiO_2 surface stabilizes the excited state, thus shifting the absorption maximum towards the lower energy of the spectrum. In our study, a shift in the absorption maximum towards higher energy of the spectrum was observed for the dye extracts adsorbed on TiO_2 . This observation suggests that there was weak adsorption of the dye extract onto TiO_2 surface which could be attributed to the high pH value and the long bond length of the OH groups present in the dye extract. The shift may also be attributed to the changing of the anthocyanin molecule from the more stable flavilium state to the unstable quinoidal state upon chelation.

It is an established fact that the light absorption by a dye monolayer is small since the cross section for photon absorption of most photosensitizers is much smaller than the geometric area occupied on the semiconductor surface, but with thin film semiconductor the obtainable LHE is usually close to unity [17]. In this work, we have used TiO_2 thin film of thickness $5.2\mu\text{m}$ and the LHE of the dye extracts and the dye mixture adsorbed onto TiO_2 surface is close to unity.

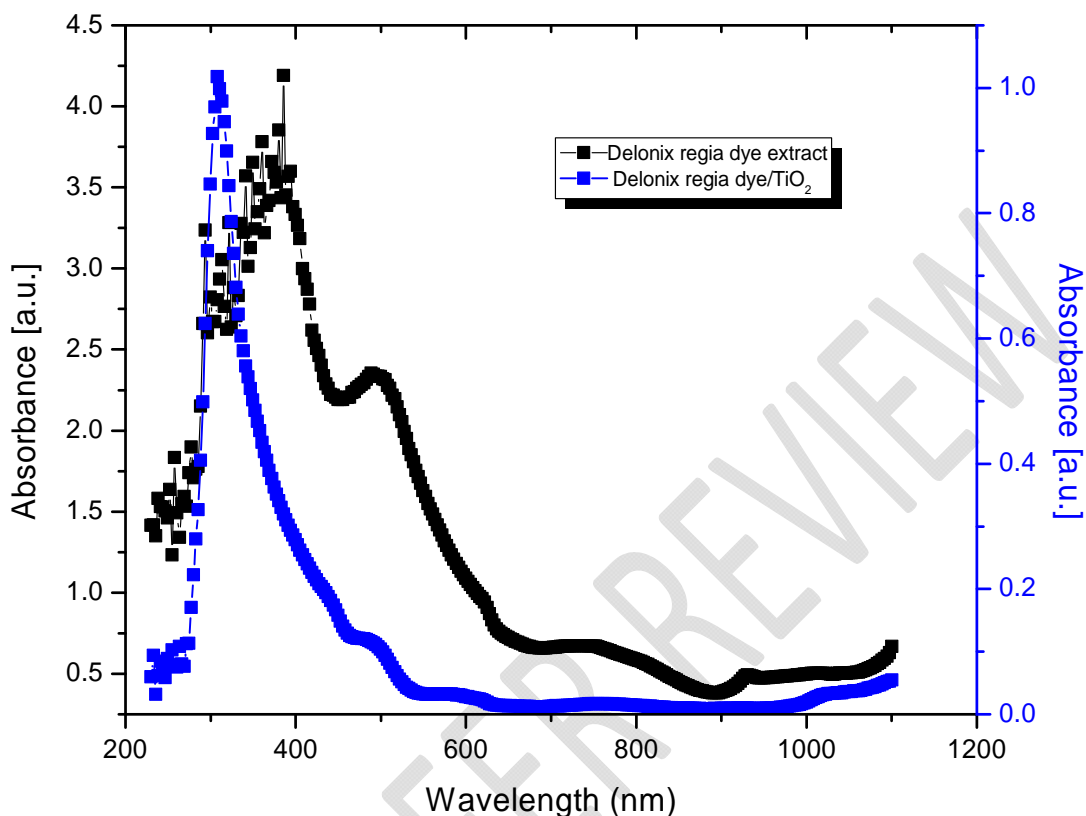


Figure 2: UV–VIS absorption spectra for Delonix regia dye extract and Delonix regia/TiO₂

The light harvesting efficiency values obtained are plotted against wavelengths as shown in figure 3. The absorption band of the dye extract on TiO₂ becomes a bit discrete after sensitization but quite broad for the dye extract. Whilst the molar extinction coefficients are very high for the dye extract on TiO₂ but it turned out that only small area is being covered by the solar irradiance spectrum. Most notably, the spectra bandwidth is within the range of 150nm to 200nm and this could be significantly enhanced if the pH is lowered using organic solvent.

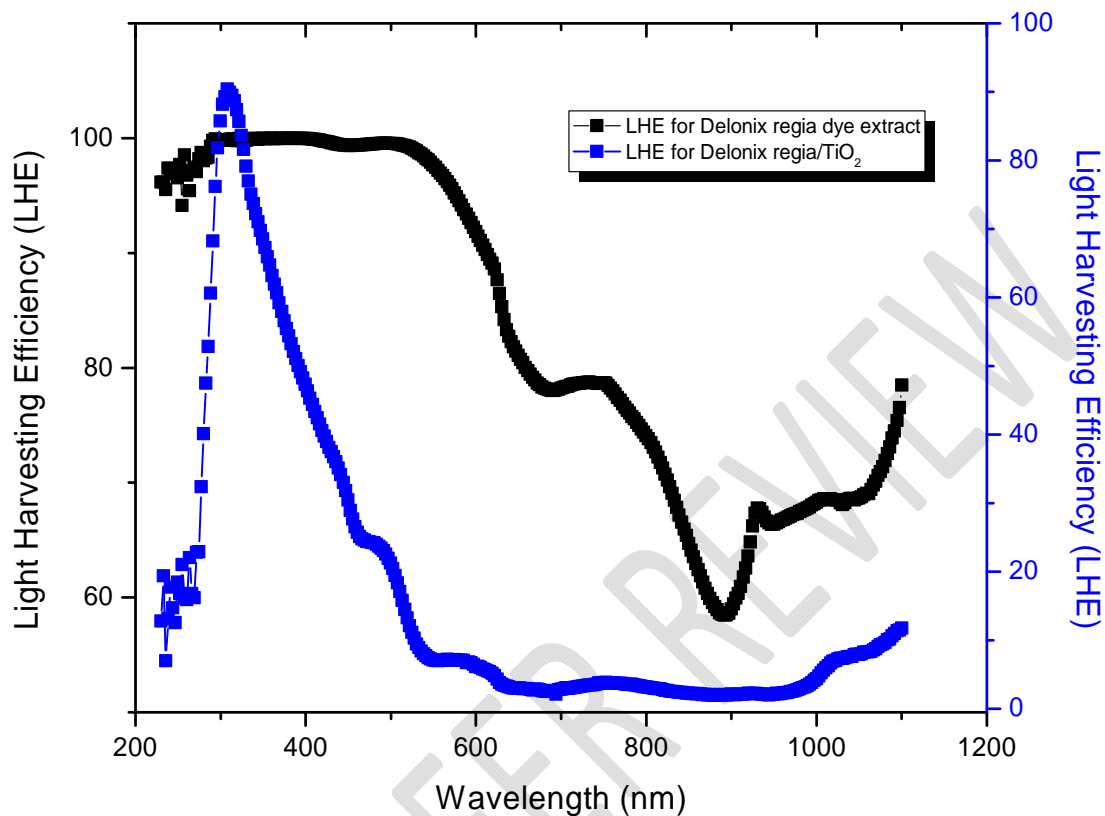


Figure 3: Light Harvesting Efficiency (LHE) for Delonix regia extract and Delonix regia/TiO₂.

The electrical characteristics for PANI determined using ECOPIA HMS-3000 (VER 3.52) are tabulated in Table 1.

Table 1: Electrical Characteristics of PANI

Bulk concentration	$3.029 \times 10^{17} \text{ cm}^{-3}$
Mobility	$1.009 \times 10^1 \text{ cm}^2 \text{ V}^{-1} \text{ s}^{-1}$
Sheet resistance	$6.050 \times 10^5 \Omega$
Resistivity	$2.043 \Omega \text{ cm}$
Magneto resistance	$9.451 \times 10^4 \Omega$
Conductivity	$4.894 \times 10^{-1} \Omega^{-1} \text{ cm}^{-1}$
Hall coefficient	$2.061 \times 10^1 \text{ cm}^3 \text{ C}^{-1}$

198

199 It is evident from table 1 that the polymeric counter electrode (PANI) is semiconducting and it is
200 a p-type semiconducting polymer with low mobility and conductivity values. The sign and the
201 value of the Hall coefficient also validate the nature of the carrier. The bulk carrier concentration
202 is $3.029 \times 10^{17} \text{ cm}^{-3}$. Current density and power versus voltage characteristics of the DSCs are
203 plotted and shown in figure 4. The photovoltaic parameters are determined and tabulated in
204 Table 2. The current density for the DSC with platinum counter electrode is 0.10 mA cm^{-2} while
205 that for the DSC with PANI counter electrode is 0.11 mA cm^{-2} . This corresponds to 10% decrease
206 in the electron recombination via redox electrolyte and collection at the photoelectrode. In the
207 same light, a 20% increase in the open circuit voltage (V_{oc}) was observed for the DSC with PANI
208 counter electrode. Since the V_{oc} of an electrochemical cell is determined by the difference
209 between the Fermi level of the semiconductor and the redox potential ($E_{f,redox}$) of the redox
210 electrolyte then, the high V_{oc} observed for the monolithic DSC suggests that this difference in the
211 Fermi levels is large. Generally the fill factor is influenced by the series resistance (R_s) arising
212 from the internal resistance and resistive contacts of the cell and shunt resistance (R_{sh}) arising
213 from the leakage of current. As such, about 37% increase in the fill factor was observed for the
214 DSC with PANI counter electrode over the DSC with platinum electrode. Approximately, 50%
215 increase in the power conversion efficiency was obtained for the DSC with PANI counter
216 electrode over the DSC with platinum electrode. Thus, it is evident from table 2 that high values
217 of J_{sc} , and V_{oc} are responsible for the higher efficiency obtained for the DSC with PANI counter
218 electrode over the DSC with platinum electrode. In our previous studies, we developed and
219 characterized DSC based on TiO_2 /Hibiscus sabdariffa/platinum electrode and the overall solar
220 power conversion efficiency of 0.033% and a maximum current density of 0.17 mA cm^{-2} were
221 obtained [5]. This boosted additional studies oriented to the use of anthocyanin dyes with
222 alternative and modified components that would lead to an enhancement in the light harvesting
223 efficiency and hence the photocurrent density which is owed to the high peak absorption
224 coefficient and large spectra bandwidth. In this work, it was discovered that TiO_2 band gap was
225 reduced upon sensitization with the dye extract. The optical band gap obtained at the point where
226 the absorption spectra showed a strong cut off, when the absorbance value is minimum is 2.40 eV .
227 The bands shift could be attributed to molecular transitions that take place when the dye

molecules chelate with TiO_2 . Typically, anthocyanin dyes exhibit $\pi - \pi^*$ orbital transition which is attributed to the wavelength range between $500nm$ to slightly above $650nm$.

Table 2: Photovoltaic parameters of DSCs sensitized with *Delonix regia* dye

DSC	$J_{sc}(mAcm^{-2})$	$V_{oc}(V)$	FF	η (%)
Movable TiO_2 - DSC with Platinum electrode	0.10	0.45	0.38	0.02
Monolithic TiO_2 -DSC with PANI electrode	0.11	0.56	0.60	0.04

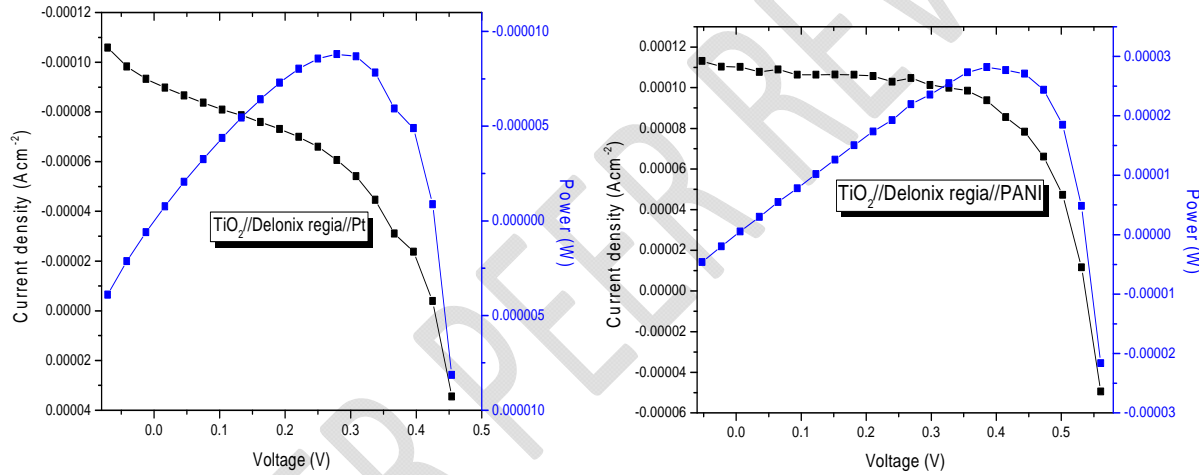


Figure 4: Current density and Power versus voltage for (a) TiO_2 -DSC//*Delonix regia* dye//Platinum electrode and (b) TiO_2 -DSC//*Delonix regia* dye//PANI electrode.

In this work, the cut off wavelength for the spectra is slightly above $600nm$. Finally, it is well known that proton adsorption causes a positive shift of the Fermi level of the TiO_2 , thus limiting the maximum photovoltage that could be delivered by the cells [15]. Nevertheless, the TiO_2 -DSC//*Delonix regia* dye//PANI electrode proved to be a better cell compared to TiO_2 -DSC//*Delonix regia* dye//Platinum electrode that exhibited lower power conversion efficiency.

However, no deviation from this trend was observed when the duration of continuous stimulated sunlight illumination was increased for several hours.

4. CONCLUSION

In this work we have reported an investigation on *Delonix regia* dye extract as natural sensitizer for TiO_2 -DSC//*Delonix regia* dye//platinum electrode and TiO_2 -DSC//*Delonix regia* dye//PANI electrode and the overall solar power conversion efficiencies of 0.02% and 0.04% were obtained respectively under AM 1.5 irradiation. *Delonix regia* dye extracts proved to be rather a poor sensitizer as can be seen by the low spectral absorption at lower energies with current density of $0.10 mA cm^{-2}$ and $0.11 mA cm^{-2}$ respectively. Nevertheless, a 10% decrease in the electron recombination via redox electrolyte and collection at the photoelectrode was observed for TiO_2 -DSC//*Delonix regia* dye//PANI electrode and a 20% increase in the open circuit voltage (V_{oc}) was also observed. Furthermore, the high V_{oc} observed for the monolithic TiO_2 -DSC//*Delonix regia* dye//PANI electrode suggests that the difference between the Fermi level of the photoelectrode and the redox potential ($E_{f,redox}$) of the redox electrolyte is large. Finally, about 37% increase in the fill factor was observed for the TiO_2 -DSC//*Delonix regia* dye//PANI electrode over TiO_2 -DSC//*Delonix regia* dye//platinum electrode. This necessitated approximately 50% increase in the power conversion efficiency for the TiO_2 -DSC//*Delonix regia* dye//PANI electrode over TiO_2 -DSC//*Delonix regia* dye//platinum electrode. Although the efficiencies obtained with this natural dye extract are still below the current requirement for large scale practical application, the results are encouraging and may boost additional studies oriented to the optimization of solar cell components compatible with the dye. In view of this, we are currently exploring the possibility of increasing the power-conversion efficiency of the DSCs based on TiO_2 using modified TiO_2 and counter electrodes and *Delonix regia*.

REFERENCES

1. Brabec CJ, Sariciftci S, Hummelen JC. Plastic Solar Cells. Advanced Functional Materials. 2001. 11, 15.

- 274 2. Ameri T, Dennler G, Lungenschmied C and Brabec J. Organic Tandem cells, Energy
275 Environ. Sci. 2009. 2, 347.
- 276
- 277 3. Li J, Grimsdale AC. Carbazole-based Polymer for Organic photovoltaic Cells. Chem.
278 Soc. Rev. 2010. 39, 2399.
- 279
- 280 4. Hagfeldt A, Boschloo G, Sun L, Kloo L, Pettersson H. Dye-sensitized Solar Cells. Chem.
281 Rev. 2010. 110(10), Pp. 6595-6663.
- 282
- 283 5. Ahmed TO, Akusu PO, ALU N, Abdullahi MB. Dye-Sensitized Solar Cells based on
284 TiO₂ Nanoparticles and Hibiscus sabdariffa. British Journal of Applied Science and
285 Technology (BJAST). 2013. 3(4); Pp.840-846.
- 286 6. Gratzel M. Dye-sensitized solar cells. Journal of Photochemistry and Photobiology C:
287 Photochemistry Reviews. 2003. 4, 145.
- 288 7. Daenke T, Kwon T, Holmes AB, Duffy NW, Bacch U, Spiccia L. High-efficiency
289 dye-sensitized solar cells with ferrocene-based electrolytes. Nature Chem. 2011. 3(3), Pp.
290 211-215.
- 291 8. Yella A, Lee H, Tsao HN, Yi C, Chandiran AK, Nazeerudin MK, Diao EW, Yeh C,
292 Zakeeruddin SM. Gratzel M. Porphyrin-Sensitized Solar Cells with Cobalt (II/III)-Based
293 Redox Electrolyte Exceed 12% Efficiency. Science. 2011. 334, 629.
- 294
- 295 9. O'Regan B, Gratzel M. A low cost, high efficiency solar cell based on dye sensitized
296 colloidal TiO₂ films. Nature. 1991. 353, 737.
- 297 10. Bach U, Lupo D, Comte P, Moser JE, Wiessortel F, Salbeck J, Spreitzer H, Gratzel M.
298 Solid-State Dye-Sensitized Mesoporous TiO₂ Solar Cells with High Photon-to-Electron
299 Conversion Efficiencies. Nature. 1998. 395, 583.
- 300
- 301 11. Diamant Y, Chen SG, Melamed O, Zaban A. Core-Shell Nanoporous Electrode for Dye
302 Sensitized Solar Cells: the Effect of the SrTiO₃ Shell on the Electronic Properties of the
303 TiO₂ Core. J. Phys. Chem. B. 2003. 107, Pp.1977-1981.
- 304 12. Sayer RA, Hodson SL, Fisher TS. Improved Efficiency of Dye-Sensitized Solar Cells
305 Using a Vertically Aligned Carbon Nanotube Counter Electrode. J. Solar Energy Engin.
306 2010. 132(2), Pp.021007-021011.
- 307 13. Rahman MM, Kojima R, Fihry ME-F, Tadaki D, Ma T, Kimura Y, Niwano M. Effect of
308 Porous Counter Electrode with Highly Conductive Layer on Dye-Sensitized Solar Cells.
309 Japanese Journal of Applied Physics. 2011. 50(8).

- 310 14. Nazeeruddin MK, Zakeeruddin SM, Humphry-Baker R, Jirousek M, Liska P,
311 Vlachopoulos N, Shklover V, Fischer CH, Gratzel M. Acid-Base Equilibria of (2,2'-
312 Bipyridyl-4,4'-dicarboxylic acid)ruthenium(II) Complexes and the Effect of Protonation
313 on Charge-Transfer Sensitization of Nanocrystalline Titania. *Inorg. Chem.* 1999. 38, Pp.
314 6298-6305.
- 315 15. Hao S, Wu J, Huang Y, Lin J. Natural dyes as photosensitizers for dye-sensitized solar
316 cell. *Solar Energy.* 2006. 80, 209.
- 317
- 318 16. Ooyama Y, Harima Y. Photophysical and electrochemical properties, and molecular
319 structures of organic dyes for dye-sensitized solar cells. *Chem. Phys. Chem.* 2012.
320 13(18); Pp.4032–80.
- 321
- 322 17. Gratzel M. Solar energy conversion by dye-sensitized photovoltaic cells. *Inorganic*
323 *Chemistry.* 2005. 44, 6841.